Cancer Chemother Pharmacol (2011) 67:349–360
DOI 10.1007/s00280-010-1323-z

ORIGINAL ARTICLE

Pharmacokinetics and pharmacodynamics of AZD6244 (ARRY-142886) in tumor-bearing nude mice

Cathrine L. Denton · Daniel L. Gustafson

Received: 16 December 2009 / Accepted: 1 April 2010 / Published online: 21 April 2010

Abstract
Purpose AZD6244 (ARRY-142886) (AstraZeneca, Macclesfield, UK) is a novel small molecule MEK1/2 inhibitor that is currently being tested in Phase II trials. With the recent publication of human pharmacokinetic data from clinical studies, we now know the achievable levels and range of AZD6244 exposure in humans. This study aimed to describe the pharmacokinetic profile of AZD6244 in mice in order to design preclinical studies that recapitulate exposure levels in humans.
Methods Male athymic, nude mice received subcutaneous inoculation of A375 human melanoma cells. Once tumors reached 400–700 mm^3, mice were given a single dose of either 5 or 10 mg/kg AZD6244 via oral gavage. Additionally, a subset of mice was dosed once daily for 1 week (10 mg/kg). Mice were killed and plasma and tissues were collected at various time points after the last dose. Samples were analyzed by LC/MS/MS for AZD6244 concentration. Additionally, pharmacodynamic endpoints such as tumor proliferation and ERK phosphorylation were analyzed at various time points after the last dose.
Results After either a single dose or at steady state, at clinically equivalent exposures, AZD6244 effectively inhibits ERK phosphorylation and suppresses proliferation. Furthermore, we describe a hysteretic relationship between the pharmacokinetics and the pharmacodynamics of AZD6244 and both target and pharmacologic responses.
Conclusions The information presented herein will drive the rational design of pre-clinical studies that are not only relevant to the clinical setting, but also pave the way to understand the biological response to AZD6244 treatment.

Keywords AZD6244 · MEK inhibitor · PK/PD relationship · Hysteresis

Abbreviations

MAPK	Mitogen activated protein kinase
PK	Pharmacokinetic
PD	Pharmacodynamic
BrdU	5-bromo-2′-deoxyuridine

Introduction

The MAPK pathway is frequently activated in human melanoma by mutations in either NRAS or BRAF [3, 7, 9, 10] that confer advantages in proliferation, migration and survival. A critical component of this pathway, located

Portions of this work were presented previously as an abstract: Denton CL, Gustafson DL (2009) AZD6244 (ARRY-142886) pharmacokinetics and pharmacodynamics in tumor-bearing nude mice. AACR Meeting Abstracts, Apr 2009; 2009: 2922.

Electronic supplementary material The online version of this article (doi:10.1007/s00280-010-1323-z) contains supplementary material, which is available to authorized users.

C. L. Denton
Animal Cancer Center, Veterinary Teaching Hospital, Colorado State University, ACC226, 300 W. Drake Rd., Fort Collins, CO 80523-1620, USA

D. L. Gustafson
University of Colorado Cancer Center, Anschutz Medical Campus, 13001 E. 17th Place, Aurora, CO 80045, USA

D. L. Gustafson (✉)
Department of Clinical Sciences, Veterinary Teaching Hospital, Colorado State University, ACC226, 300 W. Drake Rd., Fort Collins, CO 80523-1620, USA
e-mail: Daniel.Gustafson@colostate.edu

downstream of NRAS and BRAF, is the mitogen activated protein kinase kinase (MEK). MEK 1/2 is an attractive target for drug therapy of melanoma because its only known substrate is ERK 1/2. Abrogation of MEK activity by small molecule inhibitors has been shown to suppress ERK 1/2 activation and lead to an inhibition of proliferation.

AZD6244 (ARRY-142886; AstraZeneca, Macclesfield, UK) is a potent, selective, MEK1/2 inhibitor. Binding of this class of molecules to the MEK protein–ATP complex prevents downstream phosphorylation of ERK1/2 and thus impedes MAPK signaling. Pre-clinical studies of AZD6244 in various mouse xenograft models have shown tumor growth stasis and in some cases, regression [2, 6, 11, 12, 21]. A recent Phase I pharmacokinetic and pharmacodynamic study of AZD6244 in humans resulted in stable disease of five or more months in 9 of 54 patients (16%). AZD6244 was well tolerated with the most common toxicity being skin rash, diarrhea, nausea and fatigue [1]. However, it is clear from this and other studies [8, 13, 17] that the use of MEK inhibitors will likely reach higher clinical efficacy when used in combination with other cancer therapeutics. In fact, pre-clinical studies testing the combination of AZD6244 with docetaxel showed an increased anti-tumor response in a mouse xenograft model [6, 11].

Although AZD6244 is being extensively studied, both clinically and pre-clinically, no comprehensive plasma and tissue pharmacokinetics studies of AZD6244 in the mouse have been published. In order to design clinically relevant pre-clinical studies, it is critical to understand both the pharmacokinetics and pharmacodynamics of AZD6244 in tumor-bearing mice. The purpose of this study was to determine the plasma and tissue pharmacokinetics of AZD6244 and how the PK/PD relationship relates to drug activity in a human melanoma xenograft model. Gaining an understanding of the pharmacokinetic and pharmacodynamic profile of AZD6244 will allow the design of pre-clinical studies that recapitulate exposure levels in humans, and furthermore, this information will drive the rational design of pre-clinical studies that are not only relevant to the clinical setting, but also pave the way to understand the biological response to AZD6244 treatment.

Materials and methods

Chemicals and reagents

AZD6244 (ARRY-142886) was a generous gift from AstraZeneca (Macclesfield, UK) and AR509 (a structural analog of AZD6244) was a generous gift from Array Biopharma (Boulder, CO, USA). All other chemicals and solvents were of reagent or higher grade and were obtained from Fisher Scientific (Pittsburgh, PA, USA) or Sigma (St. Louis, MO, USA).

Cells

A375 human melanoma cell lines were obtained from Gail Eckhardt, MD (University of Colorado Cancer Center). Cells were maintained in RPMI medium with 300 mg L^{-1} L-glutamine (Mediatech Inc., Herndon, VA, USA) and supplemented with 10% fetal bovine serum (Mediatech) and 1 U mL^{-1} penicillin and 100 μg mL^{-1} streptomycin (HyClone, Logan, UT, USA). Cells were maintained in a humidified atmosphere at 37°C in 5% CO_2.

Xenografts

Six to eight weeks-old BALB/c athymic nude mice were purchased from the National Cancer Institute (Frederick, MD, USA). Animals were housed in polycarbonate cages, and kept on a 12-h light/dark cycle with food and water given ad libitum. All of the studies were conducted in accordance with the National Institutes of Health "Principles of laboratory animal care" (NIH publication No. 85-23, revised 1985) guidelines for the care and use of laboratory animals, and animals were housed in a facility accredited by the American Association for Accreditation of Laboratory Animal Care. Animals were allowed to acclimate for 7 days before any handling.

A375 human melanoma cells were harvested and resuspended in a 4:1 mixture of serum-free RMPI 1640 and Matrigel (BD Bioscience, Bedford, MA, USA). Five million cells were injected subcutaneously into the rear flank using a 20-gauge needle. Tumor volumes, measured by digital calipers, were calculated by Eq. 1 [20]

$$V\left(\mathrm{mm}^3\right) = 0.5 \times \left(\mathrm{length} \times \mathrm{width}^2\right) \quad (1)$$

Tumors were allowed to grow up to 400–600 mm^3 before initiating dosing.

Single dose mouse study

AZD6244 for p.o. administration was made as a suspension in sterile filtered 1% Tween 80 in PBS by vortexing briefly. Mice with tumors that had reached a volume of at least 400 mm^3 were given a single dose of 5 or 10 mg/kg AZD6244 by p.o. gavage. Gavage volumes varied between 94 and 140 μL based on animal weight (4 μL/g body weight). Mice were given a single IP injection of 200 mg/kg 5-bromo-2′-deoxyuridine (BrdU, 10 mg/mL in 0.9% sterile saline) 1 h before killing. After drug dosing, four mice per treatment group were killed at 0.5, 1, 2, 4, 8, 12 and 24 h

by cardiac stick exsanguinations under isofluorane anesthesia, and plasma and tissue samples were collected (liver, lung, kidney, gut, muscle, skin, and tumor). Collected samples were rinsed in phosphate buffered saline and immediately frozen in liquid nitrogen and stored at −80°C before sample preparation for drug analysis. Additional tumor samples were fixed in formalin for immunohistochemistry (IHC).

Daily dose mouse study

Daily dosing study was carried out in the same way as the single dose study, except that tumors were at least 600 mm^3 and mice were given a dose of 10 mg/kg AZD6244 by p.o. gavage once daily for 1 week. Four mice were killed at each of the following time points: 1, 4, 8, 12, and 24 h.

LC/MS/MS analysis of AZD6244 and *N*-desmethyl AZD6244

Analysis of AZD6244 and *N*-desmethyl AZD6244 in mouse plasma and tissues was performed using liquid chromatography tandem mass spectrometry analysis. Tissue samples were dispersed at 100 mg/mL in water by sonication. Either 100 μL of tissue suspension or 100 μL of plasma were used for the extraction. 10 μg/mL of the internal standard AR509 (structural analog, Array Biopharma, Boulder, CO, USA) was added to each sample, followed by 100 μL of 100% acetonitrile, and 20 μL of methanol. Samples were then vortexed for 10 min followed by centrifugation at 10,000 rpm for 10 min. The supernatant was collected for LC/MS/MS analysis.

The HPLC system consisted of an Agilent 1200 Series binary pump SL, vacuum degasser, thermostatted column compartment SL (Agilent Technologies, Santa Clara, CA, USA) and a CTC Analytics HTC PAL System autosampler (Leap Technologies, Carrboro, NC, USA). The HPLC column was a Waters Xbridge Phenyl column (4.6 × 50 mm I.D., 2.5 μm bead size) (Waters Corporation, Milford, MA, USA) protected by a SecurityGuard™ C18 cartridge (4 × 2.0 mm I.D.) (Phenomenex, Torrance, CA, USA) and maintained at room temperature. The mobile phase consisted of an aqueous component (A) of 10 mM ammonium acetate and an organic component (B) of acetonitrile. The 3.25-min run consisted of the following linear gradient elution: 80% A and 20% B at 0 min, 10% A and 90% B at 1.75 min, 10% A and 90% B at 2.5 min, 80% A and 20% B at 2.75 min and 80% A and 20% B at 3.25 min. The system operated at a flow rate of 1.0 mL/min. An aliquot of 10 μL of the supernatant was injected into the LC/MS/MS system for analysis.

Mass spectrometric detection was performed on an API 3200™ triple quadrupole instrument (Applied Biosystems Inc., Foster City, CA, USA) using multiple reaction monitoring (MRM). Ions were generated in positive ionization mode using an electrospray interface. AZD6244 compound-dependent parameters were as follows: declustering potential (DP), 30 V; entrance potential (EP), 5 V; collision cell entrance potential (CEP), 35 V; collision energy (CE), 40 V; and collision cell exit potential (CXP), 5 V. *N*-desmethyl AZD6244 compound-dependent parameters were as follows: DP, 30 V; EP, 3.5 V; CEP, 17 V; CE, 45 V; and CXP, 4.9 V. AR509 (internal standard) compound-dependent parameters were as follows: DP, 30 V; EP, 8 V; CEP, 115 V; CE, 32 V; and CXP, 6 V. Source-dependent parameters were as follows: nebulizer gas (GS1), 50 psi; auxiliary (turbo) gas (GS2), 60 psi; turbo gas temperature (TEM), 625°C; collision-activated dissociation (CAD) gas (nitrogen), 6 psi; curtain gas (CUR), 50 psi; ionspray voltage (IS), 4,500 V; and interface heater (IH), 100°C. Peak areas ratios obtained from MRM of AZD6244 (*m*/*z* 459 → 301), *N*-desmethyl AZD6244 (*m*/*z* 445 → 287) and AR509 (*m*/*z* 414 → 352) were used for quantification. The accuracy and precision (%CV) for analysis of mouse plasma were 91.4 ± 6.7 and 7.3%, respectively. The accuracy and precision for analysis of tumor tissue was 92.6 ± 4.1 with a %CV of 4.4%. All other tissues analyzed had accuracy and precision values similar to plasma and tumor.

Western blot

Frozen tumor samples were disrupted by sonication at a concentration of 20 mg/mL in Lysis Buffer [(150 mM NaCl, 10 mM Tris (pH 7.5), 0.2 mM Na-Orthovanadate, 1% Triton-X, 3.5 mg/mL PMSF, 0.2% Protease Inhibitor Cocktail (Sigma)]. Total cellular protein was determined via BCA Assay (Pierce, Rockford, IL). Equal amounts of total cellular protein were resolved by SDS-PAGE and transferred onto PVDF membranes. Blots were blocked for 1 h at room temperature and probed with primary at 4°C overnight. Anti-ERK and anti-phospho-ERK primary antibodies were obtained from Cell Signaling Technology (Danvers, MA). After incubation with horseradish peroxidase-conjugated donkey-anti-rabbit secondary antibody (Santa Cruz Biotechnology), proteins were detected using ECL Plus chemiluminescence kit (GE Healthcare, Pittsburgh, PA). Blots were imaged using a Typhoon Imager (Amersham Biosciences, Piscataway, NJ). Pixel intensity AUCs for ERK 1/2 and phospho-ERK 1/2 were generated using ImageJ Analysis Software v.1.41 (NIH, Bethesda, MD, http://rsb.info.nih.gov/ij/index.html). Percentage Inhibition was calculated as follows:

$$\% \text{ pERK Inhibition} = 100 \times \left(1 - \left[\left(\text{Treated}_{(\text{AUC}-\text{pERK}/\text{AUC}-\text{ERK})}\right) / \left(\text{Vehicle}_{(\text{AUC}-\text{pERK}/\text{AUC}-\text{ERK})}\right)\right]\right)$$

Immunohistochemistry

Formalin fixed tumor samples were embedded in paraffin and 5 μm sections were cut and mounted on glass slides. Sections were deparaffinized using xylene and alcohol. Antigen retrieval was performed using Antigen Unmasking Solution (Vector Laboratories, Burlingame, CA, USA) per manufacturer directions, in a decloaking chamber. Endogenous peroxidases were blocked using 3% hydrogen peroxide. For BrdU staining, slides were then incubated in 2 N HCl for 20 min, and then neutralized using 0.1 M Borate buffer, pH 8.5. BrdU sections were blocked for 10 min at 37°C using Sniper Blocking reagent (Vector Laboratories) and then probed with anti-BrdU primary antibody (DakoCytomation, Denmark) for 1 h at 37°C. Slides were incubated in Envision + Dual Link System secondary (DakoCytomation). BrdU-positive cells were visualized using DAB. TUNEL sections were processed as per manufacturer's instructions for In Situ Cell Death Detection Kit, TMR Red (Roche Diagnostics, Mannheim, Germany). Hematoxylin and Eosin (H&E) stained slides were prepared by the Diagnostics Lab at the Colorado State University Veterinary Teaching Hospital. BrdU, TUNEL and H&E stained sections were imaged using a Zeiss Axioplan 2 imaging e fluorescent microscope and AxioVision Rel 4.6 software (Carl Zeiss Microimaging Inc., Thornwood, NY, USA). Coded slides were then scored using AxioVision automated software and/or scoring by hand.

Pharmacokinetic and statistical analysis

Analysis of data for the calculation of plasma pharmacokinetic parameters was carried out using noncompartmental analysis with WinNonlin v. 5.2 (Pharsight Corp., Mountain View, CA, USA). Tissue pharmacokinetic parameters were determined using MS Office Excel 2007 (Microsoft Corp., Redmond, WA, USA). Area under the concentration–time curves (AUCs) were calculated using the trapezoidal rule; the elimination rate constant (k_{el}) was calculated using the following formula: $k_{el} = (\ln C_2 - \ln C_1)/t_2 - t_1$; the half-life ($t_{1/2}$) was calculated as $0.693/k_{el}$. One-way ANOVA with Tukey's post test statistical analyses were carried out using Prism v. 5.01 (GraphPad Software Inc., San Diego, CA, USA).

Results

Single dose pharmacokinetics

Initially, single dose pharmacokinetic profiles of AZD6244 (Fig. 1a) in tumor-bearing nude mice were characterized at two doses. The A375 human melanoma cell line was used because it harbors the BRAF-V600E mutation that is frequently found in human melanoma clinical samples as well as in cell lines [7, 10, 15, 16]. Mice were administered a single oral dose of AZD6244 at either 5 or 10 mg/kg. Plasma and tissue samples were collected from four mice

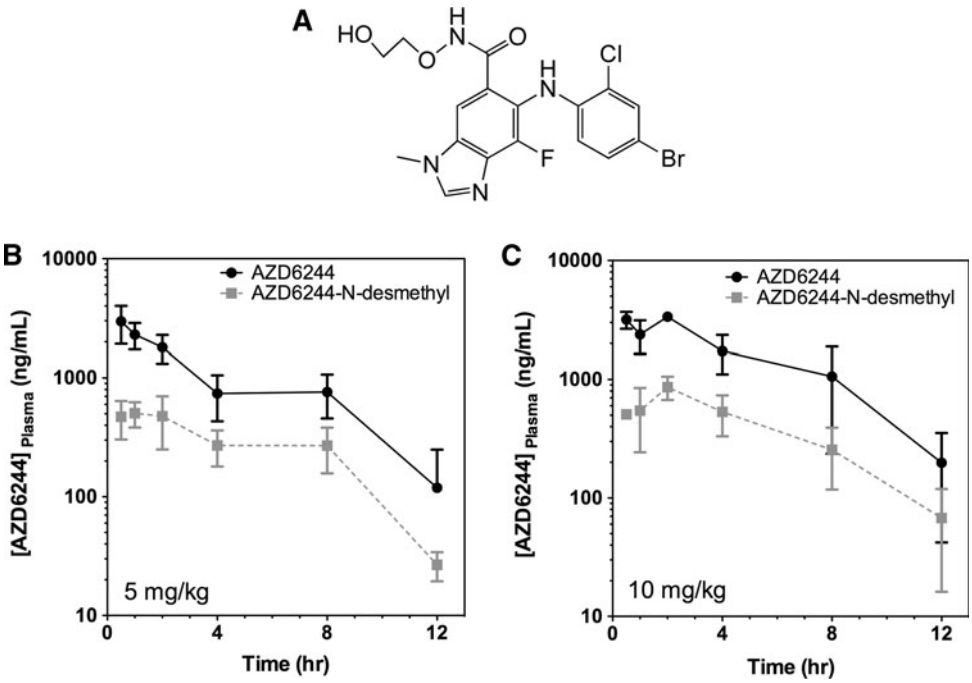

Fig. 1 AZD6244 chemical structure and single dose plasma pharmacokinetics. **a** AZD6244 structure. **b**, **c** Plasma concentration versus time curves of AZD6244 and the metabolite, AZD6244-*N*-desmethyl. Tumor-bearing mice were administered a single oral dose of AZD6244 at either **b** 5 or **c** 10 mg/kg (mean, SD, $n = 4$)

per time point after dosing. Because AZD6244 is metabolized via *N*-demethylation to an active compound that inhibits cellular growth in vitro at approximately twice the potency of the parent (data not shown), we decided to measure *N*-desmethyl-AZD6244 as well. Plasma concentrations of AZD6244 and the active metabolite, AZD6244-*N*-desmethyl were measured, and the single dose plasma pharmacokinetic results are shown in Fig. 1. Pharmacokinetic parameters for AZD6244 (Table 1) and AZD6244-*N*-desmethyl (Table 2) were calculated using noncompartmental methods. The area under the curve ($AUC_{0-24\ h}$) and C_{max} values increased with dose. T_{max} for the 5 mg/kg dose was at 0.5 h with an immediate decline in plasma AZD6244 concentration. However, for the 10 mg/kg dose, the plasma AZD6244 concentration showed a plateau from 0.5 to 2 h, suggesting protracted absorption potentially due to limited dissolution. Elimination half-life ($t_{1/2\gamma}$), clearance (Cl/*F*) and volume of distribution (V_z/F) remained the same for both doses indicating that dose level does not affect elimination of AZD6244 (Table 1). Interestingly, if halved, the $AUC_{0-24\ h}$ for both doses was in close proximity to the reported $AUC_{0-12\ h}$ in humans given either 100 and 200 mg AZD6244 free-base suspension BID [3,124 and 5,234 ng/(mL h)] [1]. In the interest of achieving a clinically relevant exposure level of AZD6244, we elected the 10 mg/kg dose for further study.

We further went onto characterize the tissue distribution of AZD6244 given as a single oral dose of 5 or 10 mg/kg. Results are shown in Fig. 2 and the pharmacokinetics of tissue distribution is summarized in Table 3. AZD6244 rapidly distributes to all tissues tested with tissue T_{max} ranging from 0.5 to 2 h post dose. AUCs in the tissues change in proportion to dose, as seen with the plasma PK. The volume of distribution (V_z/F) for the 5 and 10 mg/kg dose is 1.7 and 2.0 L/kg, respectively, indicating that AZD6244 does not distribute readily to the tissues, however, what drug reaches tissues is highly bound. In other words, the ratio of free drug in plasma to free drug in tissue ($f_B/f_T = 1.8$) implies that the drug in the tissues is highly bound. Furthermore, the AZD6244 AUC_{plasma} to AUC_{tissue} ratio ranged from 2.27 in rapidly perfused liver to 27.33 in slowly perfused muscle. This data suggests that AZD6244 distributes to the tissues in a manner consistent with perfusion, but that rapid clearance from the plasma prevents accumulation of drug in tissues.

Daily dose pharmacokinetics

Clinically, AZD6244 is dosed orally twice daily [1], so, in order to mimic clinical daily dosing and reach steady state, we next characterized the plasma pharmacokinetics and tissue distribution of AZD6244 given daily for 7 days. Plasma and tissue samples were collected at 1, 4, 8, 12 and 24 h after the last dose. Figure 3 shows the multiple-dose, steady state plasma and tissue pharmacokinetic results. Plasma pharmacokinetic parameters for AZD6244 and AZD6244-*N*-desmethyl are shown in Tables 1 and 2. Also shown is the tissue distribution of AZD6244 dosed daily for 7 days (Table 3). The plasma pharmacokinetic parameters of the daily dose are similar to the single dose of the drug (Fig. 4; Table 1) indicating that there is no accumulation of drug in mice when given orally every 24 h, which is consistent with the relatively short half-life and elimination of virtually all of the previous dose prior to a subsequent dose. Notably, the AUC in mice after 1 week of

Table 1 AZD6244 mouse and human plasma pharmacokinetics

	C_{max} (ng/mL)	T_{max} (h)	AUC[a] [ng/(mL h)]	$T_{1/2\gamma}$ (h)	Cl/*F* [L/(h kg)]	V_z/F (L/kg)
5 mg/kg Single dose mouse	2,968	0.5	11,910	2.81	0.4	1.7
10 mg/kg Single dose mouse	3,353	2.0	18,976	2.62	0.5	2.0
10 mg/kg Steady state mouse	2,977	1.0	17,525	2.29	0.6	1.9
100 mg Single dose human[b]	807	1.0	3,124	4.5	–	–
100 mg Steady state human[b]	895	1.0	5,006	–	–	–

[a] Adjei et al. [1]

[b] Mouse, $AUC_{0-24\ h}$; Human, $AUC_{0-12\ h}$, except Hyd-Sulfate formulation $AUC_{0-24\ h}$

Table 2 AZD6244-*N*-desmethyl mouse plasma pharmacokinetics

	C_{max} (ng/mL)	T_{max} (h)	$AUC_{0-24\ h}$ [ng/(mL h)]	$T_{1/2\gamma}$ (h)
5 mg/kg Single dose mouse	505	1.0	3,597	3.68
10 mg/kg Single dose mouse	865	2.0	4,993	2.79
10 mg/kg Steady state mouse	554	1.0	3,709	2.37

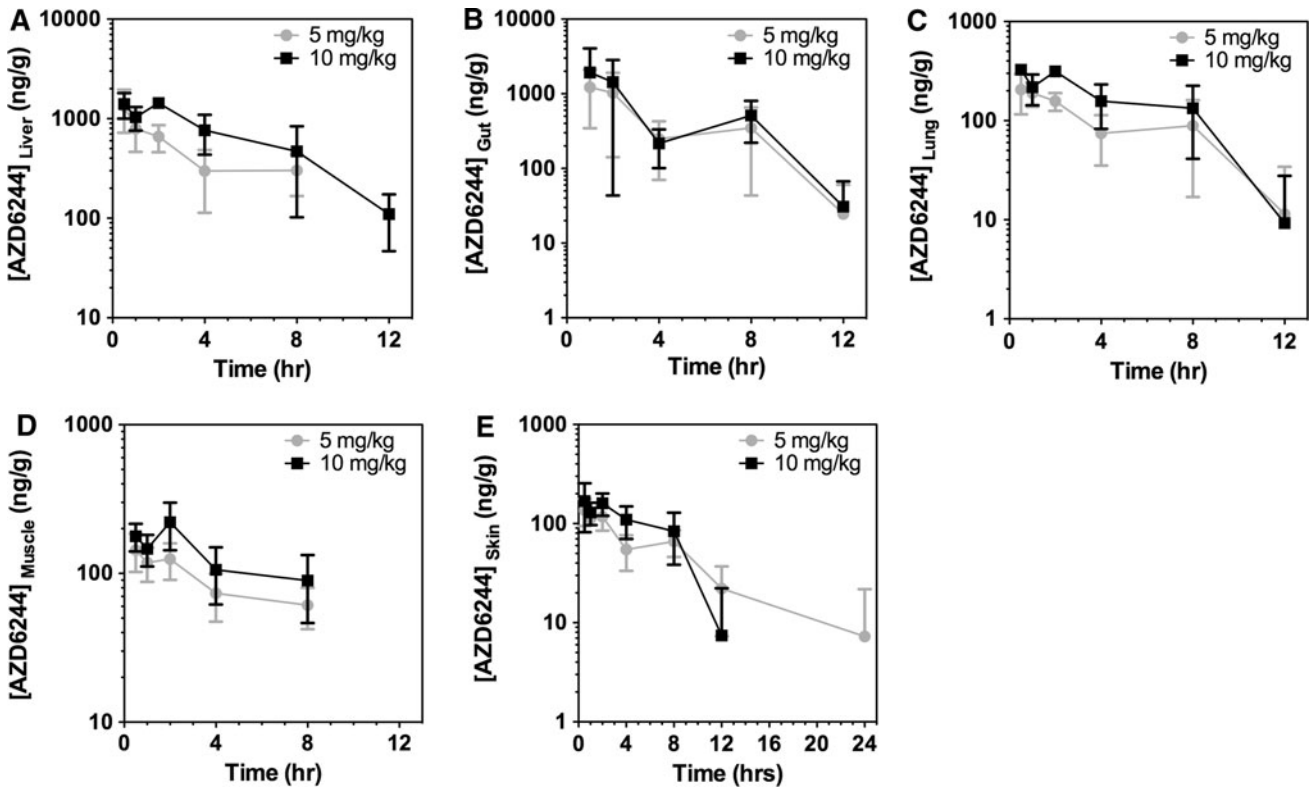

Fig. 2 Single dose tissue pharmacokinetics. AZD6244 tissue concentration versus time in **a** liver, **b** gut, **c** lung, **d** muscle and **e** skin. Tumor-bearing mice were administered a single oral dose of AZD6244 at either 5 or 10 mg/kg (mean, SD, $n = 4$)

Table 3 AZD6244 tissue distribution

Tissue	Dose (mg/kg)	Regimen	$AUC_{0-12\ h}$ [ng/(g h)]	C_{max} (ng/g)	C_{min} (ng/g)	$t_{1/2}$ (h)	$P:T_{AUC}$
Tumor	5	SD	3,601	501	44	2.9	3.17
	10	SD	4,776	861	130	3.7	3.82
	10	SS	3,795	487	52	7.6	4.45
Liver	5	SD	4,356	1,337	299	3.5	2.62
	10	SD	8,028	1,438	110	2.7	2.27
	10	SS	6,781	1,052	100	2.5	2.49
Gut	5	SD	5,008	1,224	25	1.1	2.28
	10	SD	6,845	1,930	31	1.0	2.66
	10	SS	2,278	6,778	54	1.5	7.41
Muscle	5	SD	813	1,436	611	5.8	14.06
	10	SD	667	2,210	896	4.6	27.33
	10	SS	930	2,044	1,649	0.6	18.16
Lung	5	SD	1,083	206	11	1.4	10.55
	10	SD	2,446	327	9	1.0	7.45
Skin	5	SD	802	136	7	2.5	14.25
	10	SD	1,101	169	7	1.2	16.56

SD single dose, *SS* steady state

once daily dosing is still in line with the clinical AUC in humans after 15 days of twice-daily dosing [1]. Tissue distribution in the daily dose regimen was similar to single dose tissue distribution indicating that AZD6244 does not accumulate in any of the tissues when given on a daily basis.

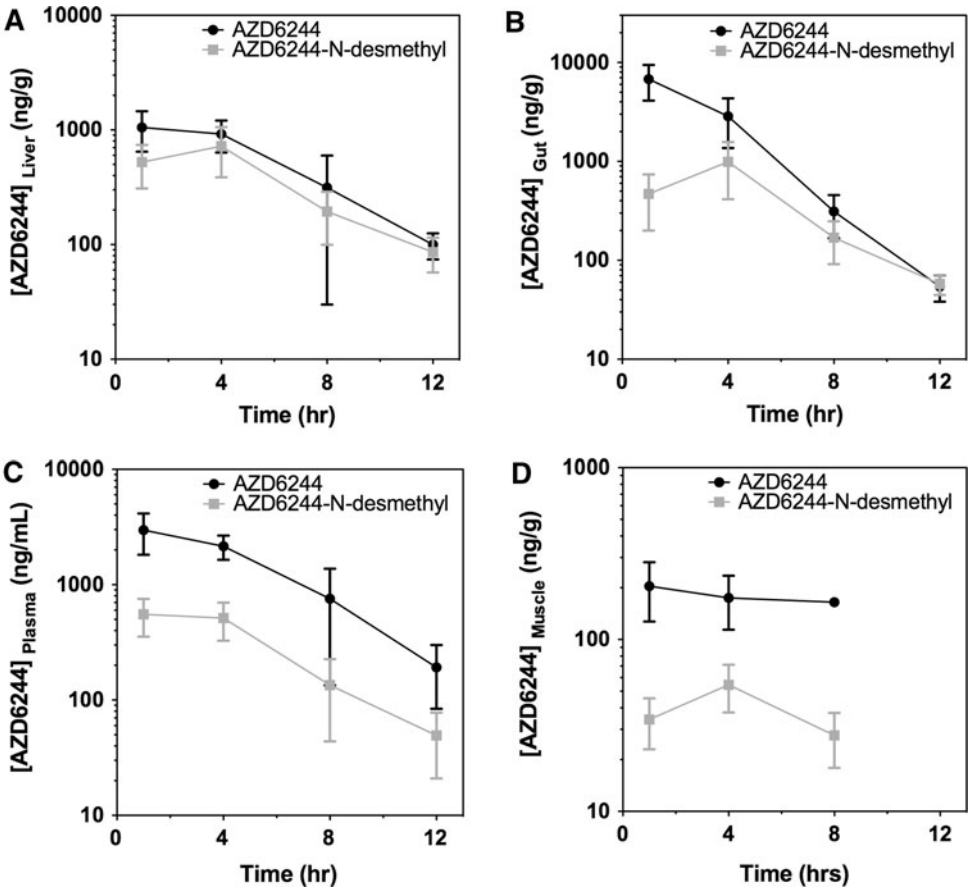

Fig. 3 Daily dose pharmacokinetics and tissue distribution. AZD6244 and AZD6244-*N*-desmetnyl concentration versus time in **a** plasma, **b** liver, **c** gut, **d** muscle. Tumor-bearing mice were administered a once daily oral dose of 10 mg/kg AZD6244 daily for 7 days. Samples were taken at the indicated time after the last dose (mean, SD, $n = 4$)

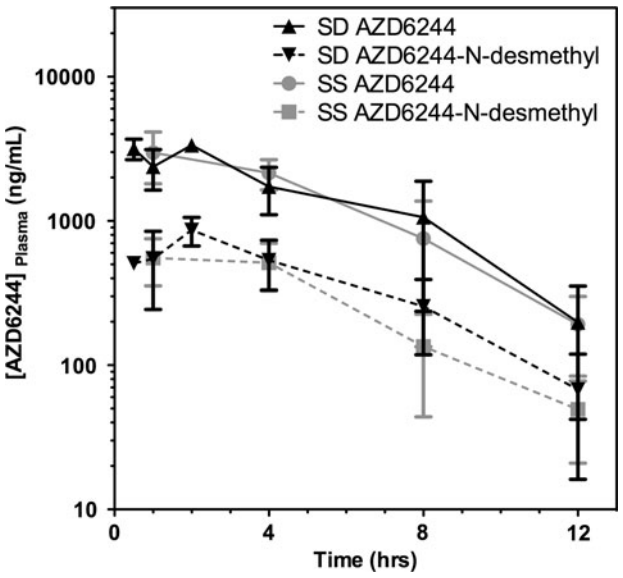

Fig. 4 Comparison of the plasma concentration versus time curves of AZD6244 and AZD6244-*N*-desmethyl for the 10 mg/kg single dose and 10 mg/kg daily dose regimens. *SD* single dose, *SS* steady state (mean, SD, $n = 4$)

Tumor pharmacokinetics and pharmacodynamics

In order to elucidate the pharmacokinetic/pharmacodynamic (PK/PD) profile of AZD6244, we further measured tumor drug concentrations of AZD6244 in subcutaneous A375 human melanoma xenografts. Tumor pharmacokinetic profiles of AZD6244 in all three dose regimens are shown in Fig. 5. Tumor AUCs and $t_{1/2}$ are shown in Table 3 and range from 3,601 to 4,776 ng/(g h) and 2.9–7.6 h, respectively. These exposure levels correspond to 0.79–1.04 μM and are well within the range seen to elicit an anti-proliferative response in the A375 cell line grown in culture (median effective dose of 42 nM). The molecular target of AZD6244 is MEK, which when bound by AZD6244 is incapable of phosphorylating ERK [21]. Therefore, as an indicator of AZD6244 target inhibition in the tumor, we measured ERK and phospho-ERK levels by western blot. Figure 5 shows the relationship between tumor AZD6244 drug levels and percent reduction of phosphorylated ERK as an indication of MEK1/2 inhibition. In the single dose regimen, at both 5 and 10 mg/kg, there is an immediate and statistically

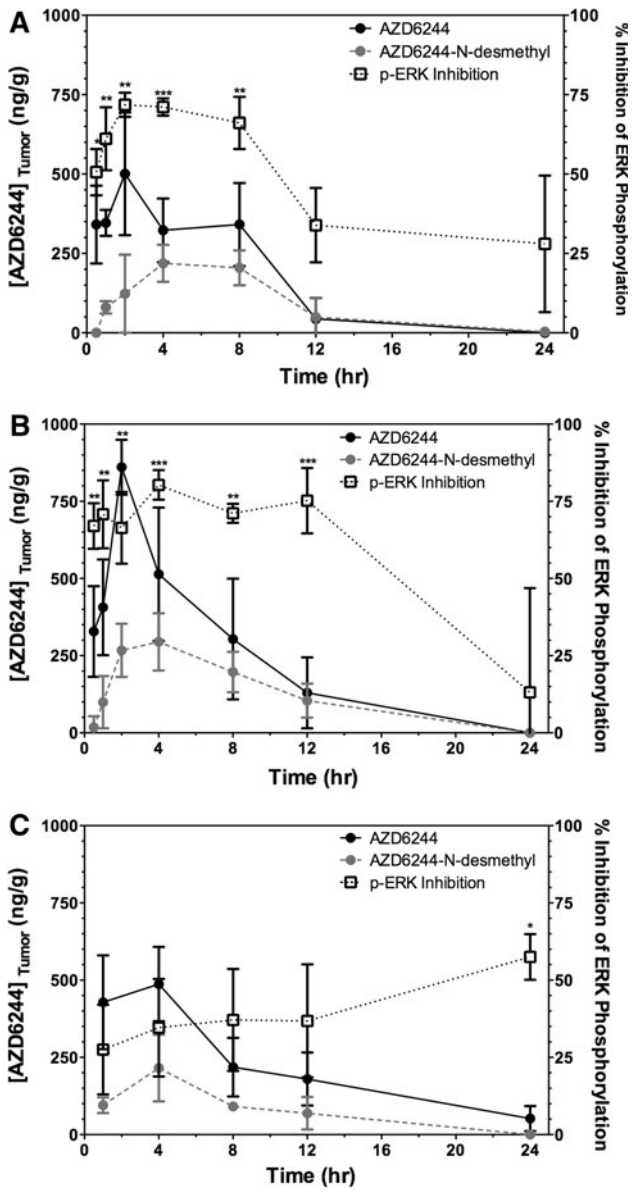

Fig. 5 Time profile comparison of inhibition of tumor ERK phosphorylation and tumor AZD6244 concentration. Mice were given a single dose of **a** 5 mg/kg, **b** 10 mg/kg, or **c** 10 mg/kg daily for 7 days. Tumor samples were taken at the indicated time after the last dose. Tumors were lysed and equal amounts of total protein were resolved by SDS-PAGE. Membranes were probed with ERK and phospho-ERK antibodies. Ratios of the pixel intensity of pERK:ERK were analyzed for % inhibition = 100 × [1 − (treated/control)] (mean, SD, $n = 4$). One-way ANOVA p values comparing each time point to control tumor as follows: *$p < 0.05$; **$p < 0.01$; ***$p < 0.001$

significant inhibition of phosphorylated ERK which peaks at 72% in the 5 mg/kg group and at 80% in the 10 mg/kg group. After a high level of inhibition that lasts between 8 and 12 h, there is a sharp decline to 20–30%, as the tumor concentration of AZD6244 decreases. Alternatively, in the mice receiving daily continuous doses of AZD6244, we observed phospho-ERK inhibition that is sustained at 28–58% through the 24-h dosing period, even as the tumor concentration of AZD6244 decreases to negligible levels. To our knowledge, this is the first characterization of the PK/PD profile of a continuous dose of AZD6244 in a mouse xenograft model and it clearly supports the efficacy of target inhibition of the 10 mg/kg daily dose.

It has been shown that inhibition of ERK phosphorylation is not the best indicator of the anti-tumor efficacy of various MEK inhibitors including AZD6244 [18, 19]. In order to clarify the anti-tumor effects of AZD6244, we next attempted to elucidate the anti-proliferative outcome by analyzing incorporation of the nucleoside analog, 5-bromo-2′-deoxyuridine (BrdU), into the tumors. BrdU incorporation indicates DNA replication and thus labels cells in S-phase. Mice treated with 5 or 10 mg/kg AZD6244 as either a single dose or 10 mg/kg daily for 7 days were administered 200 mg/kg BrdU 1 h before killing. As shown in Fig. 6, after either a single dose (Fig. 6a, b) or after continuous dosing (Fig. 6c) of AZD6244, there is a clear reduction in S-phase cells as compared to control. Notably, the continuous dose group exhibits a sustained inhibition of S-phase that ranges between 39 and 71% of control. This inhibition of S-phase is the greatest between 8 and 12 h for all dose groups, but begins to return to near-normal levels by 24 h after the last dose. Interestingly, in the daily dose group, S-phase inhibition not only is sustained, but also is significantly different from control groups at 1 and 8 h post dose (one-way ANOVA, Tukey's PT). The differing pharmacodynamic profile for BrdU of the acute versus the daily dose regimens is due to chronic and sustained pharmacological inhibition of proliferation that overlaps the 24 h dosing interval despite the daily rise and fall of AZD6244 concentrations in the tumor.

Finally, to further characterize the in vivo pharmacological effects of AZD6244 in A375 human melanoma xenograft tumors, we analyzed tumor sections for apoptosis and necrosis. Although there was a slight increase in apoptotic cells as measured by TUNEL, this increase was not statistically significant (Supplemental Fig. 1A). Furthermore, there was no difference in necrotic area between the vehicle and AZD6244 treated tumors (Supplemental Fig. 1B). These results indicate that, in this tumor model, the pharmacological outcome of AZD6244 is limited to reduction in tumor cell proliferation rather than an increase in tumor cell death.

AZD6244 pharmacokinetic/pharmacodynamic relationship

Understanding the in vivo pharmacology of AZD6244 is critical to achieve optimal use in the clinic and designing rational combinations for further testing. Therefore, we

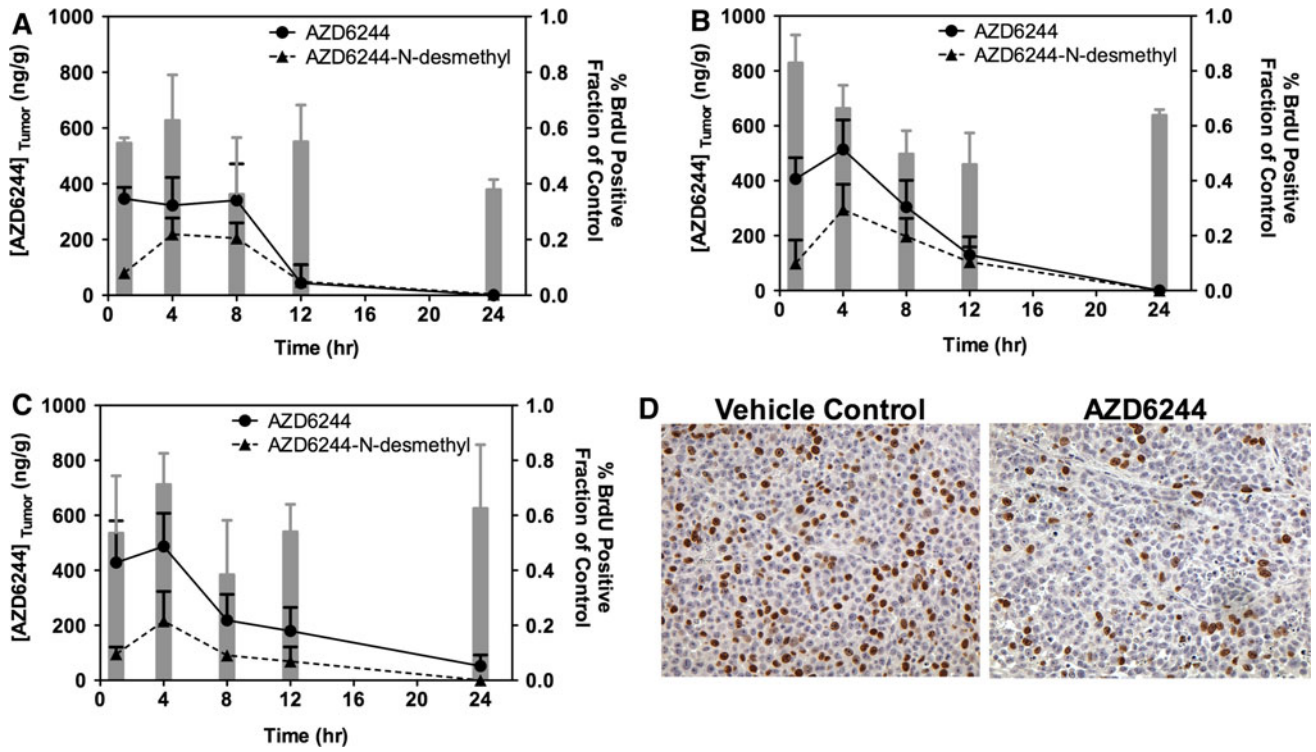

Fig. 6 Time profile comparison of tumor proliferation as measured by BrdU incorporation and tumor AZD6244 concentration. Mice were given **a** a single dose of 5 mg/kg, **b** a single dose of 10 mg/kg or **c** 10 mg/kg daily for 7 days. Tumor samples were taken at the indicated time after the last dose, fixed in formalin and mounted on glass slides. Immunohistochemistry for BrdU was performed and blinded slides were scored (mean, SD, $n = 3$, One-way ANOVA p values comparing each time point to control tumor as follows: $*p < 0.05$; $**p < 0.01$; $***p < 0.001$). **d** Representative images of tumor sections from vehicle- and AZD6244-treated mice

next explored the pharmacokinetic/pharmacodynamic relationship of AZD6244 to target inhibition as measured by decreasing ERK phosphorylation and the subsequent signaling pathway inhibition leading to downstream decrease in proliferation. As shown in Fig. 7, AZD6244 displays clear hysteresis in both pathway inhibitions (Fig. 7a) and inhibition of proliferation (Fig. 7c). Classic hysteresis, observed here in both Fig. 7a, c, indicates a time lag between drug concentration and pharmacologic effects in the tumor (hysteresis reviewed in [4, 5, 14]). We propose a schematic representation of this relationship in Fig. 7d. This schematic depicts a time lag between plasma concentrations of AZD6244 and inhibition of ERK in tumor due to diffusion of drug from plasma to tumor, i.e. the diffusion time lag. The time lag due to diffusion of AZD6244 into the tumor is reinforced by the resulting linear relationship between tumor AZD624 concentration and inhibition of ERK phosphorylation (Fig. 7b, $r^2 = 0.7359$). This diffusion time lag is subsequently followed by another time lag between tumor concentrations of AZD6244 and inhibition of proliferation due to the changes in the signaling molecules (i.e. MEK inhibition) and the transduction of these changes down the signaling cascade that result in pharmacologic response, i.e. the signaling time lag.

Discussion

In this study, we describe the plasma and tissue pharmacokinetics of AZD6244 and resulting PK/PD relationships relating to drug activity in a human melanoma xenograft model. We show that in order to achieve AZD6244 exposures in mice similar to those in clinical use, the appropriate dose is 10 mg/kg given by oral gavage, once daily. This dosing regimen achieves an AUC of 17,525 ng/(mL h) which is comparable to the human AUC of 10,012 ng/(mL h) [1]. Furthermore, we show that this dosing regimen results in sustained inhibition of the MAP kinase pathway leading to suppression of proliferation.

It is important to note that because the half-life of AZD6244 is short, there is nearly complete clearance from plasma and tissues at the end of the 24-h dosing

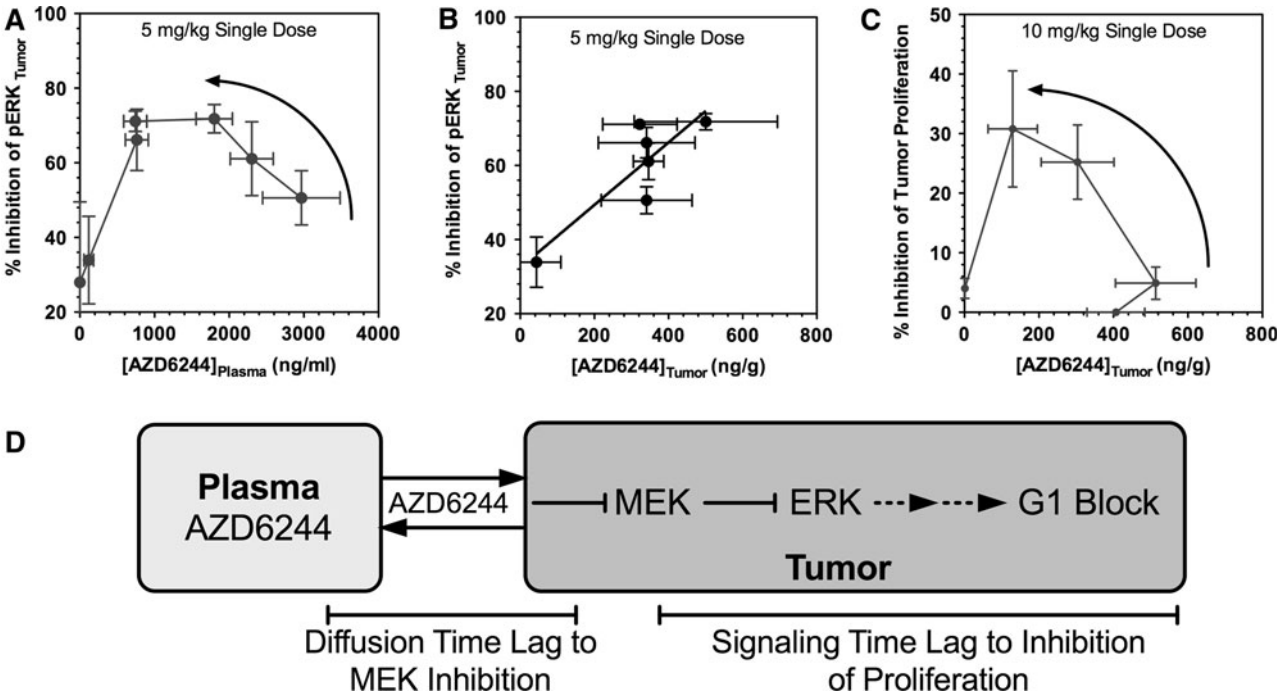

Fig. 7 AZD6244 shows hysteretic PK/PD relationships. **a** % inhibition of tumor ERK phosphorylation versus plasma (AZD6244) ng/mL; **b** % inhibition of tumor ERK phosphorylation versus tumor (AZD6244) ng/mL; **c** % inhibition of tumor proliferation versus tumor (AZD6244) ng/g; and **d** schematic representation of AZD6244 PK/PD relationships to cell signaling and proliferation (mean, SEM, $n = 3$)

period. This results in little to no accumulation of drug in the course of daily dosing. However, markers of drug action in the tumor show sustained inhibition of proliferation that lasts throughout the 24-h period, thus achieving a sustained pharmacodynamic effect even though drug levels decline. The pharmacokinetic-pharmacodynamic relationship of AZD6244 in human tumors has not been established, although it is clear that proliferation is suppressed [1].

Various studies have shown that analyzing phospho-ERK inhibition as a measure of target modulation by MEK inhibitors such as AZD6244 is not the best measure of the anti-tumor efficacy of these agents [18, 19]. In our study, we see a strong, significant inhibition of phospho-ERK in all of the dosing regimens tested. Furthermore, when we explored the anti-proliferative effects via the more direct measure of BrdU incorporation into cells undergoing S-phase, there was a strong and sustained inhibition of proliferation in the steady state group. To our knowledge, this is the first comprehensive pharmacodynamic analysis of tumor-specific AZD6244 drug action and pharmacokinetics.

An interesting effect elucidated by this study is the different pharmacodynamic profiles of AZD6244 when given as either a single acute dose, or as a protracted continuous daily dose. In the acute dosing regimen, the nadir of proliferation appeared to be at around 8–12 h. However, the protracted regimen results in a dip in proliferation immediately after dosing. We believe that this may be due to a sequencing effect on the tumor cells. In the presence of AZD6244 given as an acute dose, cycling cells are blocked as they enter G1-phase, which may take few hours as all the cells in the tumor are in different stages of the cell cycle upon the first dose. However, under protracted exposure to AZD6244, the pharmacological inhibition of proliferation is maintained throughout the dosing interval, such that upon re-exposure to AZD6244 every 24 h, there is no interruption of drug effects. Finally, we show, for the first time, the hysteretic relationship between AZD6244 in plasma and target effect in tumor (diffusion time lag), and the hysteretic relationship between AZD6244 and pharmacologic effect (signaling time lag). Understanding this relationship may be important for achieving optimal use of AZD6244 in the clinic and designing rational combinations with other targeted agents, chemotherapy or radiation.

In summary, we have presented a comprehensive pharmacokinetic and pharmacodynamic profile for AZD6244. By understanding the non-linear and time-dependent relationship between the plasma pharmacokinetics and the tumor pharmacodynamics of AZD6244, we hope to design more accurate and relevant pre-clinical studies.

Specifically, since AZD6244 appears to be an excellent agent for the sequencing of tumor cells in the cell cycle, and because although cytotoxic effects are observed in some pre-clinical models [6], it is more commonly cytostatic, we expect the information presented here to assist in the design and implementation of combination studies with chemotherapy. Furthermore, it may be necessary when administering AZD6244 clinically to give a drug holiday in order to mitigate adverse events such as rash. This drug holiday would provide the opportunity for the careful sequencing of chemotherapeutics to achieve a more enhanced anti-tumor response. We believe that in this context, AZD6244 can be used as a powerful tool in the treatment of melanoma.

Acknowledgments We thank Dr. Paul Smith for critical review of this manuscript and for providing intellectual support. Funding for this work was provided by a National Institutes of Health Grant, CA101988-05.

Conflict of interest statement None.

References

1. Adjei AA, Cohen RB, Franklin W, Morris C, Wilson D, Molina JR, Hanson LJ, Gore L, Chow L, Leong S, Maloney L, Gordon G, Simmons H, Marlow A, Litwiler K, Brown S, Poch G, Kane K, Haney J, Eckhardt SG (2008) Phase I pharmacokinetic and pharmacodynamic study of the oral, small-molecule mitogen-activated protein kinase kinase 1/2 inhibitor AZD6244 (ARRY-142886) in patients with advanced cancers. J Clin Oncol 26:2139–2146
2. Ball DW, Jin N, Rosen DM, Dackiw A, Sidransky D, Xing M, Nelkin BD (2007) Selective growth inhibition in BRAF mutant thyroid cancer by the mitogen-activated protein kinase kinase 1/2 inhibitor AZD6244. J Clin Endocrinol Metab 92:4712–4718
3. Brose MS, Volpe P, Feldman M, Kumar M, Rishi I, Gerrero R, Einhorn E, Herlyn M, Minna J, Nicholson A, Roth JA, Albelda SM, Davies H, Cox C, Brignell G, Stephens P, Futreal PA, Wooster R, Stratton MR, Weber BL (2002) BRAF and RAS mutations in human lung cancer and melanoma. Cancer Res 62:6997–7000
4. Csajka C, Verotta D (2006) Pharmacokinetic-pharmacodynamic modelling: history and perspectives. J Pharmacokinet Pharmacodyn 33:227–279
5. Danhof M, Visser SA (2002) Pharmaco-electroencephalography and pharmacokinetic-pharmacodynamic modeling in drug development: focus on preclinical steps. Methods Find Exp Clin Pharmacol 24(Suppl D):127–128
6. Davies BR, Logie A, McKay JS, Martin P, Steele S, Jenkins R, Cockerill M, Cartlidge S, Smith PD (2007) AZD6244 (ARRY-142886), a potent inhibitor of mitogen-activated protein kinase/extracellular signal-regulated kinase kinase 1/2 kinases: mechanism of action in vivo, pharmacokinetic/pharmacodynamic relationship, and potential for combination in preclinical models. Mol Cancer Ther 6:2209–2219
7. Davies H, Bignell GR, Cox C, Stephens P, Edkins S, Clegg S, Teague J, Woffendin H, Garnett MJ, Bottomley W, Davis N, Dicks E, Ewing R, Floyd Y, Gray K, Hall S, Hawes R, Hughes J, Kosmidou V, Menzies A, Mould C, Parker A, Stevens C, Watt S, Hooper S, Wilson R, Jayatilake H, Gusterson BA, Cooper C, Shipley J, Hargrave D, Pritchard-Jones K, Maitland N, Chenevix-Trench G, Riggins GJ, Bigner DD, Palmieri G, Cossu A, Flanagan A, Nicholson A, Ho JW, Leung SY, Yuen ST, Weber BL, Seigler HF, Darrow TL, Paterson H, Marais R, Marshall CJ, Wooster R, Stratton MR, Futreal PA (2002) Mutations of the BRAF gene in human cancer. Nature 417:949–954
8.. Dummer R, Robert C, Chapman PB, Sosman JA, Middleton M, Bastholt L, Kemsley K, Cantarini MV, Morris C, Kirkwood JM (2008) AZD6244 (ARRY-142886) vs temozolomide (TMZ) in patients (pts) with advanced melanoma: an open-label, randomized, multicenter, phase II study. J Clin Oncol 26:15S
9. Edlundh-Rose E, Egyhazi S, Omholt K, Mansson-Brahme E, Platz A, Hansson J, Lundeberg J (2006) NRAS and BRAF mutations in melanoma tumours in relation to clinical characteristics: a study based on mutation screening by pyrosequencing. Melanoma Res 16:471–478
10. Goel VK, Lazar AJ, Warneke CL, Redston MS, Haluska FG (2006) Examination of mutations in BRAF, NRAS, and PTEN in primary cutaneous melanoma. J Invest Dermatol 126:154–160
11. Haass NK, Sproesser K, Nguyen TK, Contractor R, Medina CA, Nathanson KL, Herlyn M, Smalley KS (2008) The mitogen-activated protein/extracellular signal-regulated kinase kinase inhibitor AZD6244 (ARRY-142886) induces growth arrest in melanoma cells and tumor regression when combined with docetaxel. Clin Cancer Res 14:10
12. Huynh H, Soo KC, Chow PK, Tran E (2007) Targeted inhibition of the extracellular signal-regulated kinase kinase pathway with AZD6244 (ARRY-142886) in the treatment of hepatocellular carcinoma. Mol Cancer Ther 6:138–146
13. Lorusso PM, Adjei AA, Varterasian M, Gadgeel S, Reid J, Mitchell DY, Hanson L, DeLuca P, Bruzek L, Piens J, Asbury P, Van Becelaere K, Herrera R, Sebolt-Leopold J, Meyer MB (2005) Phase I and pharmacodynamic study of the oral MEK inhibitor CI-1040 in patients with advanced malignancies. J Clin Oncol 23:5281–5293
14. Mager DE, Wyska E, Jusko WJ (2003) Diversity of mechanism-based pharmacodynamic models. Drug Metab Dispos 31:510–518
15. Omholt K, Platz A, Kanter L, Ringborg U, Hansson J (2003) NRAS and BRAF mutations arise early during melanoma pathogenesis and are preserved throughout tumor progression. Clin Cancer Res 9:6483–6488
16. Poynter JN, Elder JT, Fullen DR, Nair RP, Soengas MS, Johnson TM, Redman B, Thomas NE, Gruber SB (2006) BRAF and NRAS mutations in melanoma and melanocytic nevi. Melanoma Res 16:267–273
17. Rinehart J, Adjei AA, Lorusso PM, Waterhouse D, Hecht JR, Natale RB, Hamid O, Varterasian M, Asbury P, Kaldjian EP, Gulyas S, Mitchell DY, Herrera R, Sebolt-Leopold JS, Meyer MB (2004) Multicenter phase II study of the oral MEK inhibitor, CI-1040, in patients with advanced non-small-cell lung, breast, colon, and pancreatic cancer. J Clin Oncol 22:4456–4462
18. Smalley KS, Contractor R, Haass NK, Lee JT, Nathanson KL, Medina CA, Flaherty KT, Herlyn M (2007) Ki67 expression levels are a better marker of reduced melanoma growth following MEK inhibitor treatment than phospho-ERK levels. Br J Cancer 96:445–449

19. Solit DB, Garraway LA, Pratilas CA, Sawai A, Getz G, Basso A, Ye Q, Lobo JM, She Y, Osman I, Golub TR, Sebolt-Leopold J, Sellers WR, Rosen N (2006) BRAF mutation predicts sensitivity to MEK inhibition. Nature 439:358–362
20. Teicher BA (2002) Tumor models in cancer research. Humana Press, Totowa
21. Yeh TC, Marsh V, Bernat BA, Ballard J, Colwell H, Evans RJ, Parry J, Smith D, Brandhuber BJ, Gross S, Marlow A, Hurley B, Lyssikatos J, Lee PA, Winkler JD, Koch K, Wallace E (2007) Biological characterization of ARRY-142886 (AZD6244), a potent, highly selective mitogen-activated protein kinase kinase 1/2 inhibitor. Clin Cancer Res 13:1576–1583